

Signal and Image Denoising in Transform Domain and Wavelet Shrinkage: A Comparative Study

¹Ruşen Öktem, ²Leonid Yaroslavsky, and ³Karen Egiazarian

^{1,3}Signal Processing Laboratory, Tampere University of Technology Tampere 33101, Finland

²Interdisciplinary Department, Engineering Faculty, Tel Aviv University, Tel Aviv 69978, Israel

¹rusen@cs.tut.fi ²yaro@eng.tau.ac.il ³karen@cs.tut.fi

ABSTRACT

In this work, nonlinear local transform domain filtering is reviewed, and its relation with wavelet denoising is discussed. A postprocessing stage is applied to a number of transform domain denoised signals to obtain a better estimate of the original signal. Simulations are made over different Gaussian noise corrupted one-dimensional signals and images, in DCT and wavelet transform domains. Their performances with respect to threshold, transform basis and window size are compared.

1 INTRODUCTION

Signal and image processing in transform domain rather than in spatial domain suggests certain advantages in terms of the convenience of incorporating a priori knowledge on signals into the design of processing algorithms and in terms of computational expenses. The transfer from signal domain into the transform domain is especially promising if it is applied locally rather than globally. In [8], local adaptive filtering in transform domain for image restoration is studied in detail. Local adaptive filters introduced in [8] work in the domain of an orthogonal transform in a moving window and nonlinearly modify the transform coefficients to obtain an estimate of the central pixel of the window. Recently, nonlinear filtering in wavelet transform domain has been introduced in terms of wavelet denoising by Donoho and Johnstone [4], and found efficient applications in restoration of different types of images ranging from medical imaging to synthetic aperture radar. In this work, we will review the design of optimal nonlinear transform domain filters and introduce a postprocessing stage. We will compare performances of local transform domain filters and wavelet denoising on additive Gaussian noise corrupted signals with respect to different parameters. We will introduce the observation model and the filter design problem in Section 2. In Section 3, we will present simulation results and finally conclude the work in Section 4.

2 TRANSFORM DOMAIN FILTERS FOR SIGNAL RESTORATION

Transform domain filtering basically consists of following three steps:

1. Computing spectral coefficients $\{\beta_{r_1, r_2}\} = \mathbf{T}\mathbf{b}$ of the observed image fragment \mathbf{b} within the window over the chosen orthogonal transform \mathbf{T} .

2. Multiplication of the obtained spectral coefficients by the filter coefficients $\{\eta_{r_1, r_2}\}$,

$$\hat{\alpha}_{r_1, r_2} = \eta_{r_1, r_2} \beta_{r_1, r_2}. \quad (1)$$

3. Inverse transformation \mathbf{T}^{-1} of the output signal spectral coefficients $\{\hat{\alpha}_{r_1, r_2}\}$,

where subscripts (r_1, r_2) are corresponding indices in the transform domain.

With this approach, by minimizing the average square error between the estimation and true value of the pixel, the filter parameters are found in [8] as

$$\eta_{r_1, r_2} = \frac{\mathbf{AV}_{imsys} \mathbf{AV}_{obj} \{\alpha_{n_1, n_2} (\beta_{r_1, r_2})^*\}}{\mathbf{AV}_{imsys} \mathbf{AV}_{obj} \{|\beta_{r_1, r_2}|^2\}}, \quad (2)$$

with $*$ denoting complex conjugate, \mathbf{AV}_{imsys} and \mathbf{AV}_{obj} denoting averaging over realizations of imaging system sensor noise and unknown parameters of the image, respectively. The design of the local adaptive filter is therefore reduced to an estimation of local power spectrum of the input image fragment and its mutual local spectrum with the 'ideal' image.

2.1 Local Adaptive Filters with Nonlinear Processing in Transform Domain

Consider an observed signal modeled by the equation

$$\mathbf{b} = \mathbf{L}\mathbf{a} + \mathbf{n}, \quad (3)$$

where \mathbf{n} is a random, zero mean signal independent noise, and \mathbf{L} is a linear operator of the imaging system. Let the distorted signal be described in the orthogonal transform domain by the relation

$$\alpha_{r_1, r_2} = \lambda_{r_1, r_2} \beta_{r_1, r_2} + \nu_{r_1, r_2}, \quad (4)$$

where λ_{r_1, r_2} are running representation coefficients of the linear operator \mathbf{L} in the orthogonal transform domain, and ν_{r_1, r_2} are zero mean spectral coefficients of the realization of the noise interference. Then, the optimum filter coefficients can be found from equation (2) as,

$$\eta_{r_1, r_2} = \frac{|\lambda_{r_1, r_2}|^2 |\alpha_{r_1, r_2}|^2}{\lambda_{r_1, r_2} \mathbf{AV}_{imsys} \mathbf{AV}_{obj} |\beta_{r_1, r_2}|^2}. \quad (5)$$

The estimation of the ‘‘ideal’’ signal fragment spectrum can be carried out by the following relationship,

$$|\lambda_{r_1, r_2}|^2 |\alpha_{r_1, r_2}|^2 \approx \max\{0, \mathbf{AV}_{imsys} \mathbf{AV}_{obj} |\beta_{r_1, r_2}|^2 - \mathbf{AV}_{imsys} |\nu_{r_1, r_2}|^2\}. \quad (6)$$

Using a zero order approximation for $\mathbf{AV}_{imsys} \mathbf{AV}_{obj}$, the following filter realization for signal denoising and deblurring is found in [8],

$$\eta_{r_1, r_2} = \begin{cases} \max\left\{0, \frac{|\beta_{r_1, r_2}|^2 - |\nu_{r_1, r_2}|^2}{\lambda_{r_1, r_2} |\beta_{r_1, r_2}|^2}\right\}, & \lambda_{r_1, r_2} \neq 0 \\ 0, & \text{else} \end{cases}, \quad (7)$$

and the following filter modification, called ‘‘**rejective**’’ filter is proposed,

$$\eta_{r_1, r_2} = \begin{cases} 1/\lambda_{r_1, r_2}, & |\beta_{r_1, r_2}|^2 \geq thr \text{ and } \lambda_{r_1, r_2} \neq 0 \\ 0, & \text{else} \end{cases}, \quad (8)$$

where the value of *thr* is associated with the variance of additive noise. Note that the idea of shrinkage of transform coefficients that are lower than a certain threshold recently reappeared and obtained popularity in the form of wavelet shrinkage [3, 4]. The nonlinear operation in transform domain defined by (8) refers to hard thresholding used in wavelet denoising.

2.2 Wavelet Denoising

Wavelet transform decomposes a signal into successive levels of resolution by use of two channel perfect reconstruction filter banks. Wavelet transform compacts most of the real signals energy in a few low resolution coefficients with high magnitude, where wavelet transform of noise spreads over all coefficients with a low magnitude. Wavelet denoising (WD) exploits this energy compaction property of the wavelet transform, and works in three steps of transform domain filtering presented in Section 2.1. In that case, the orthogonal transform \mathbf{T} is chosen as the wavelet transform which operates on the whole data by use of filter banks, rather than operating on a sliding window, and filter coefficients are as given in Eq.8 or Eq.7 with $\lambda_{r_1, r_2} = 1$. Although wavelet denoising does not operate on a sliding window, but on the overall image, localization property of wavelet transform makes it possible to consider local behaviour of the data. Nonlinear wavelet methods for recovery of signals is studied in detail by Donoho [2]. However, wavelet denoising introduces artifacts (undershoots and overshoots) to the denoised signal. Those

artifacts are studied and translation invariant denoising to obtain better performance have been proposed in [2]. Translation invariant (TI-WD) denoising performs signal recovery in the following steps: 1. Perform wavelet denoising both on the noisy signal and circularly shifted versions of the noisy signal; 2. unshift the denoised shifted signals and 3. average over the results obtained. Since a discrete wavelet transform is shift variant, the artifacts in filtered output of shifted signal do not appear at the same locations as the filtered output of nonshifted signal. Hence, averaging over shifts result in elimination of artifacts that appear in wavelet denoising.

2.3 A Postprocessing Stage to Local Transform Domain Denoising

In subsection 2.1, a sliding window over the signal is used to estimate the central pixel value. Although this local transform approach with a sliding window is expected to adapt the local characteristics of the signal better than global transform domain approach, it may still result in similar artifacts encountered in wavelet denoising. To obtain a similar effect as translation invariant denoising does, it is possible to keep the denoising results for every pixel in a window and estimate a pixel’s value by averaging the corresponding pixel’s outputs from denoising of several windowed fragments. Let $W_{k, l}$ be the $N \times N$ window enclosing the pixels $(k, l), \dots, (k + N - 1, l + N - 1)$. The denoised value of pixel $(r_1, r_2) \in W_{k, l}$ by applying a denoising operator to the fragment of signal enclosed by $W_{k, l}$ can be expressed as

$$\hat{a}_{r_1, r_2}^{(k, l)} = [\mathbf{T}^{-1}(\{\eta_{i, j} \cdot \beta_{i, j}\})], \quad (i, j) \in W_{k, l}. \quad (9)$$

An estimation of pixel (r_1, r_2) can be obtained by

$$\hat{a}_{i, j} = \frac{1}{N^2} \sum_{k=r_1-N+1}^{r_1} \sum_{l=r_2-N+1}^{r_2} \hat{a}_{r_1, r_2}^{(k, l)}, \quad (10)$$

$$k = r_1 - N + 1, \dots, r_1, \quad l = r_2 - N + 1, \dots, r_2.$$

We call the overall transform domain nonlinear filtering with the postprocessing stage introduced by equations (9-10) as transform domain averaged local filter (ALCF).

3 COMPARATIVE RESULTS

The reviewed transform domain filters and introduced transform domain averaged local filter are tested on two one dimensional signals, an ECG signal and a piecewise constant signal of length 1024 with range $\{-1, 1\}$, and on 256×256 images, two aerospace images *aero1* and *aero2*, the Lenna image, an MRI image and a piecewise constant image. Gaussian noise with standard deviation $\sigma = 0.1$ is added to one dimensional signals resulting in $MAE_{ecg} = 0.0818$, $MAE_{piecewise} = 0.0802$. Noisy images are obtained by adding Gaussian noise of standard deviation $\sigma = 15$.

DCT, Daubechies 4 (Db4) wavelet basis, and Haar basis with different window sizes are used to obtain transform domain signals. Both wavelet transform and DCT are appropriate in terms of obtaining accurate spectrum estimation from the observed data and in terms of computational complexity. DCT in a running window can be computed recursively, [5]. Hard thresholding (Eq.8) is tested with several threshold values. In Figure 3 (Left), RMSE variation of the compared methods with respect to threshold are presented for denoised ECG signal. It shows that averaging over several denoising results provides better robustness to threshold. In Figure 3 (Right), PSNR variation of averaged local filter with DCT basis with respect to window size and threshold is presented for Lena image. The transform window length which gives the optimum result depends on the characteristics of the signal.

Quantitative results are tabulated in Table 1, where $RMSE = \sqrt{MSE}$, and $PSNR = 10 \log_{10}(255^2/MSE)$. They show that local transform domain filtering with sliding window performs better than wavelet denoising. Although quantitative results for translation invariant denoising and averaged local transform domain denoising are comparable, visual results (see Figures 1, 2) show that averaged local transform domain denoising gives better visual quality. Transform basis which results in the best performance depend on the signal structure, i.e., Haar basis performs better than Daubechies for piecewise constant signals.

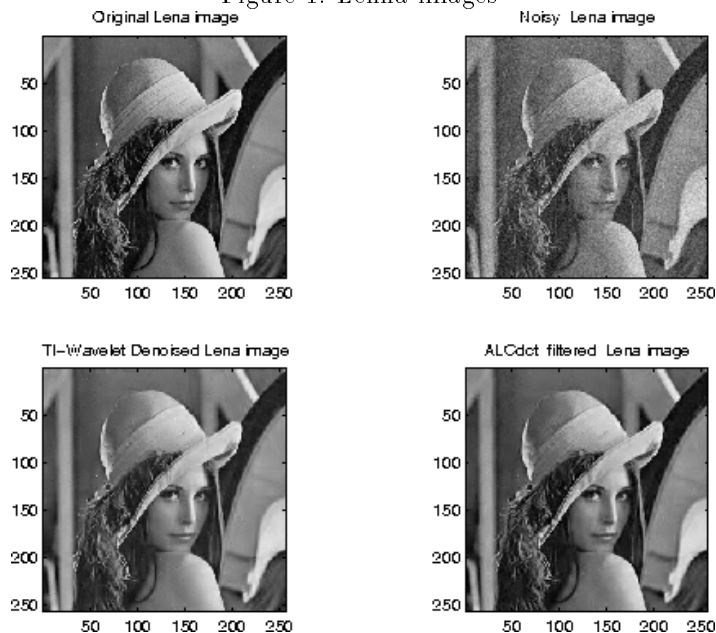
4 CONCLUSIONS

We reviewed nonlinear filter implementations in orthogonal transform domain and compared their performance with respect to several parameters like window size, transform basis, and threshold. We compared performance of wavelet denoising, translation invariant wavelet denoising and transform domain filtering within a sliding window over a signal. We found out that averaging the denoising results of local transform domain denoising within a range of windowed signals (instead of using one window to estimate its central pixel) increases both the visual and quantitative performance. Future extension of this work may include using different estimators than a simple averaging over the range of denoising outputs of windowed signals. It is also concluded that window size which results in the best output in local filtering depends on the image structures. Hence, using a varying sized window may be included in the future work as well.

References

[1] M.R. Branham, A.K. Katsaggelos, "Digital Image Restoration", *IEEE Signal Processing Magazine*, pp. 24-41, March 1997.
 [2] R.R. Coifman, D.L. Donoho, "Translation- Invariant De-Noising", *Wavelets and Statistics*, Anestis

Figure 1: Lena images



Antoniadis, ed. Springer-Verlag Lecture Notes, 1995.

[3] D.L. Donoho, "Nonlinear Wavelet Methods for Recovery of Signals, Densities, and Spectra from Indirect and Noisy Data", *Proceedings of Symposia in Applied Mathematics*, American Mathematical Society, v. 00, pp. 173-205, 1993.
 [4] D.L. Donoho, I.M. Johnstone, "Ideal Spatial Adaptation by Wavelet Shrinkage", *Biometrika*, 81(3), pp. 425-455, 1994.
 [5] K.O. Egiazarian, "Running Discrete Orthogonal Transforms and Block Adaptive LMS Digital Filters", *AMSE Review*, vol. 6, No. 3, pp. 19-29, 1988.
 [6] L. Yaroslavsky, "Digital Signal Processing in Optics and Holography", *Radio i Svyaz*, Moscow, 1987 (in Russian).
 [7] L. Yaroslavsky, M. Eden, *Fundamentals of Digital Optics*, Birkhauser, Boston, 1996.
 [8] L. Yaroslavsky, "Local Adaptive Image Restoration and Enhancement with the Use of DFT and DCT in a Running Window", *Proceedings, Wavelet Applications in Signal and Image Processing IV*, SPIE Proc. Series, v. 2825, pp. 1-13, 6-9 August 1996, Denver, Colorado.

Table 1: Quantitative results for one dimensional signals and images

Transforms	Signals				Images				
	ECG		piecewise		Lenna	piecewise	aero1	aero2	MRI
	RMSE	MAE	RMSE	MAE	PSNR	PSNR	PSNR	PSNR	PSNR
WD-haar	0.0602	0.0423	0.0419	0.0238	26.72	30.03	26.91	32.28	30.87
WD-Db4	0.0519	0.0381	0.0520	0.0352	27.16	27.78	27.57	33.28	31.50
TI-WD-haar	0.0382	0.0270	0.0218	0.0139	29.77	32.49	30.04	34.90	33.75
TI-WD-Db4	0.0354	0.0260	0.0354	0.0235	30.09	30.80	30.37	35.17	34.16
LChaar	0.0521	0.0332	0.0366	0.0220	27.36	29.50	28.14	34.16	31.82
LCdct	0.0404	0.0281	0.0555	0.0385	27.96	27.80	28.99	34.60	32.69
ALCHaar	0.0426	0.0312	0.0218	0.0142	29.64	33.49	29.78	35.11	33.54
ALCdb4	0.0352	0.0246	0.0389	0.0281	29.95	31.82	30.23	35.31	33.80
ALCdct	0.0339	0.0243	0.0439	0.0303	30.49	31.03	30.82	35.70	34.65

Figure 2: *Left* : ECG plots from up-to-down left-to-right; a.original, b.noisy, filtered with c.LChaar, d.LCdct, e.WD-Db4, f.TI-WD-Db4, g.ALCdct, h.ALCdb4. *Right* : Enlarged window from *Left* a,f,g.

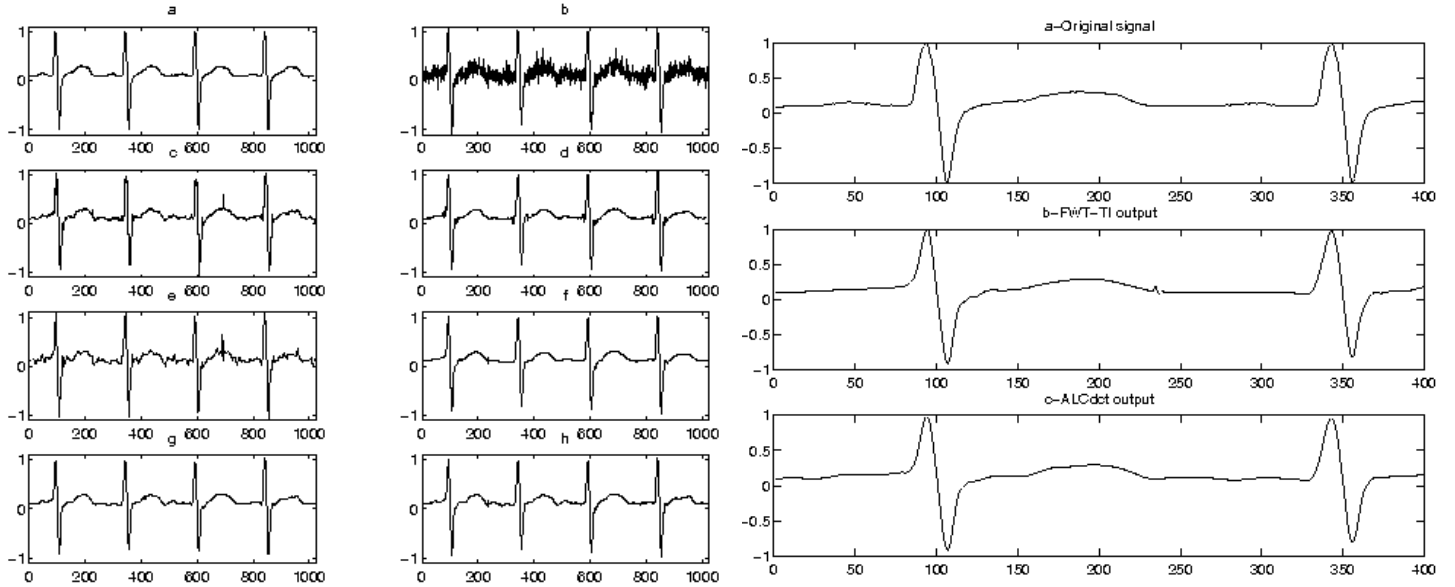


Figure 3: *Left* : Performance variation of different methods with respect to threshold. *Right* : Performance variation of ALCdct filter with respect to threshold and window sizes $w \times w$.

